Subtropical catastrophe: Significant loss of low-mode tidal energy at 28.9°

J. A. MacKinnon and K. B. Winters

Scripps Institution of Oceanography, University of California, San Diego, California, USA

Received 29 April 2005; revised 29 June 2005; accepted 6 July 2005; published 6 August 2005.

[1] An idealized numerical study of a northward propagating internal tide reveals a dramatic loss of energy to small-scale subharmonic instabilities near 28.9°N. Inspired by observations of the internal tide radiating northward from the Hawaiian Ridge, a three-dimensional numerical model is initialized with a northward baroclinic tidal flux of approximately 1.7 kW/m. After an initial spinup period, energy is quickly transferred from the baroclinic tide to subharmonic motions, with half the horizontal tidal wavenumber and small vertical scales, through nonlinear advection of horizontal tidal velocity gradients. Potential oceanic implications are twofold. First, once a steady-state has been reached, the instability acts as a partial filter of northward tidal flux between 27.5 and 29.5°N, in rough agreement with some altimetric tidal observations. Second, elevated shear of the subharmonic motions suggests the potential for elevated near-surface dissipation rates near the critical latitude that may be important for upper ocean mixing. **Citation:** MacKinnon, J. A., and K. B. Winters (2005), Subtropical catastrophe: Significant loss of low-mode tidal energy at 28.9°, *Geophys. Res. Lett.*, *32*, L15605, doi:10.1029/2005GL023376.

1. Introduction

[2] Breaking internal waves, whose energy is primarily provided by the wind and the tides, are the dominant source of deep-ocean mixing. The conversion of the barotropic tide to internal waves over rough topography provides 0.7 to 0.9 TW of the approximately 2.1 TW total energy input that *Munk and Wunsch* [1998] argue is required to maintain the abyssal stratification. A portion of the energy is extracted from the barotropic tide and dissipated within turbulent boundary layers flanking topographical features, producing a pattern of near-bottom mixing hotspots that mirrors maps of barotropic to baroclinic tidal conversion. Several recent studies suggest that inclusion of such a pattern of tidal mixing hotspots may have a pronounced influence on global abyssal flow patterns [*Hasumi and Suginohara*, 1999; *Simmons et al.*, 2004a; *Saenko and Merryfield*, 2005].

[3] Yet mixing hotspots near tidal conversion sites are only half the story. Between 50% and 95% of the available baroclinic energy escapes the nearfield to propagate up to thousands of kilometers across ocean basins [*St. Laurent and Nash*, 2004]. For example, of the estimated 25 GW extracted from the barotropic tide near Hawaii (E. D. Zaron and G. D. Egbert, Estimating open-ocean barotropic tidal dissipation: The Hawaiian Ridge, submitted to *Journal of Physical Oceanography*, 2005), only approximately 15% is dissipated locally (J. Klymak, personal communication, 2005), leaving the rest to propagate away as a low mode internal tide. Where and by what mechanism the bulk of this energy is converted to turbulent mixing is unknown.

[4] Away from sharp topographic features, the internal tide is subject to nonlinear interactions with motions at other spatial scales and temporal frequencies. Previous studies have proposed that this mechanism is not a significant sink for tidal energy. For example, *Olbers and Pomphrey* [1981] calculate that it would take months for nonlinear resonant triad interactions to transfer a significant percentage of energy out of a mode-one internal tide, and disqualified them as an important mechanism.

[5] However, several pieces of recent evidence suggest that the issue be revisited. Numerical studies suggest that Parametric Subharmonic Instability (PSI), a particular class of nonlinear interactions, is capable of rapidly transferring energy from an internal tide to smaller-scale waves of half the tidal frequency [*Hibiya et al.*, 1998, 2002; J. A. MacKinnon and K. Winters, Tidal mixing hotspots governed by rapid parametric subharmonic instability, submitted to *Journal of Physical Oceanography*, 2005, hereinafter referred to as MacKinnon and Winters, submitted manuscript, 2005]. Observations of tidal and subharmonic motions near strong tidal generation sites made during the Hawaiian Ocean Mixing Experiment (HOME) experiment also suggestively point to active PSI. For example, *Rainville and Pinkel* [2005a] see a subharmonic (near-diurnal) energy flux that waxes and wanes with the strength of the local semi-diurnal internal tide and is inconsistent with diurnal forcing. *Carter and Gregg* [2005] observe a strong and distinct high-mode subharmonic wave that biharmonic analysis reveals to be phase coupled with the radiating internal tide.

[6] One of the most important features of PSI is that it is only possible when the subharmonic frequency (one cycle per 24.8 hours) is within the internal-wave frequency band – greater than the local inertial frequency. This condition is only met equatorward of 28.9°, which we will refer to as the critical latitude. *Nagasawa et al.* [2002] and *Hibiya and Nagasawa* [2004] describe observations showing enhanced subharmonic shear near tidal generation sites equatorward but not poleward of this latitude.

[7] Satellite altimetry provides a global view of low-mode internal tide generation and propagation. *Kantha and Tierney* [1997] detect the surface signature of the first-mode semidiurnal (M_2) internal tide propagating north from Hawaii until roughly 30°N, at which point they

0094-8276/05/2005GL023376$05.00

observe a steady decrease in tidal energy flux. Also using altimetry to study the tide eminating from Hawaii, *Ray and Cartwright* [2001] see an abrupt decrease in northward tidal flux just south of 30° near 170°W and a more gradual decrease of tidal flux with increasing latitude farther west. This loss of altimetric signal could result either from dynamical processes (such as PSI) that transfer energy from the internal tide to other motions, or from localized mechanisms that alter tidal phase. On the other hand, northward tidal fluxes, presumably emanating from Hawaii, have been detected in a tomographic array [*Dushaw et al.*, 1995] and historical mooring records (M. Alford, personal communication, 2005) as far north as 40°, although the signals are weaker and highly erratic.

[8] Here we present results of a numerical study of an idealized mode-one internal tide, inspired by observations of the tide propagating north from the Hawaiian Island Chain. We find the tide to experience a catastrophic loss of energy near 28.9°, and postulate that PSI becomes particularly efficient near this critical latitude.

2. Numerical Methods

[9] The numerical model used here is more fully described by *Winters et al.* [2004] and MacKinnon and Winters (submitted manuscript, 2005). The model solves the equations of motion in an incompressible, rotating ocean with arbitrary forcing,

$$\begin{aligned}
\frac{\partial u}{\partial t} &= -\vec{u}\cdot\nabla u + f(y)v - \frac{1}{\rho_0}\frac{\partial p'}{\partial x} + \boldsymbol{\nu_p}\cdot\nabla^p u + F_u \\
\frac{\partial v}{\partial t} &= -\vec{u}\cdot\nabla v - f(y)u - \frac{1}{\rho_0}\frac{\partial p'}{\partial y} + \boldsymbol{\nu_p}\cdot\nabla^p v + F_v \\
\frac{\partial w}{\partial t} &= -\vec{u}\cdot\nabla w - \frac{1}{\rho_0}\frac{\partial p'}{\partial z} - \frac{g\rho'}{\rho_0} + \boldsymbol{\nu_p}\cdot\nabla^p w + F_w \\
\frac{\partial \rho'}{\partial t} &= -\vec{u}\cdot\nabla\rho' - w\frac{\partial\bar{\rho}}{\partial z} + \boldsymbol{\kappa_p}\cdot\nabla^p\rho' + \kappa\frac{\partial^2\bar{\rho}}{\partial z^2} + F_{\rho'} \\
\nabla\cdot\vec{u} &= 0, \qquad (1)
\end{aligned}$$

where $[u, v, w]$ is the velocity vector, ρ' is the density perturbation from a linearly increasing average density profile $[\bar{\rho}(z)]$, p' is the perturbation pressure, and ρ_0 is a reference density. The equations are solved in a rectangular domain of size [L_x = 3300 km, L_y = 3300 km (15 to 45°N), L_z = 4 km] with [N_x = 32, N_y = 512, $1N_z$ = 128] evenly spaced grid points, horizontally periodic boundary conditions, free-slip top and bottom boundary conditions, and constant stratification [$N = 2 \times 10^{-3}$ s^{-1}]. The Coriolis frequency increases linearly with latitude, $f(y) = \beta y$. Near the northern edge of the computational domain, a sponge layer is applied to damp the outgoing waves, enabling the use of horizontally periodic boundary conditions.

[10] The coefficients ($\boldsymbol{\nu_p}$, κ_p) and exponent (p) of the hyperviscosity terms in (1) are chosen to maximize the range of inviscid wavenumbers while removing energy from the smallest resolved scales quickly enough to maintain numerical stability. In practice, energy is drained from vertical scales smaller than 150 m on timescales shorter than one day. Based upon these equations we define a 'hyperdissipation' rate ϵ (henceforth simply referred to as the dissipation rate), that describes the rate at which energy is transferred to unresolved scales ($\lambda_z \ll 150$ m) by the inviscid dynamics at resolved ($\lambda_z \geq 150$ m) scales [*Winters et al.*, 2004].

[11] The experiments start from rest, and are subsequently forced so as to excite a field of northward propagating mode-one internal waves of tidal (M_2) frequency. The forcing amplitude was chosen to produce northward tidal energy fluxes of 1.7 kW/m, consistent with observations made during the HOME experiment [*Rainville and Pinkel*, 2005a]. Random, low-level background noise (rms displacement amplitude of 1 mm) is excited by adding spectrally white forcing in wavenumber space at each time step.

3. Results

[12] As the simulation begins, the mode-one tide propagates northward from the forcing region and is eventually absorbed in the high-latitude sponge layer. As the flow spins up, an instability develops near 28.9°N (Figure 1a). The instability has small vertical scale (approximately thirty times smaller that of the internal tide, remarkably similar to the subharmonic signal observed by *Carter and Gregg* [2005]), a horizontal wavenumber about half that of the internal tide, and half the tidal frequency (Figure 1).

[13] After approximately a year of spinup, a steady state is achieved in which the instability acts as an effective filter of northward tidal energy flux (Figure 1a). Between 27.5 and 29.5° the steady-state northward tidal energy flux drops from 1.6 to 0.6 kW/m. Some of the generated subharmonic energy escapes southward in the form of propagating high-mode subharmonic (locally near-inertial) internal waves (Figure 1a). However, most of the generated subharmonic energy dissipates locally. In the strongest patches, turbulent dissipation rates and associated diapycnal diffusivities are elevated several orders of magnitude above the background levels typically observed in the open ocean (Figure 1b) [*Gregg*, 1998]. The surprising strength of this energy loss leads us to refer to the phenomenon as a 'Subtropical Catastrophe'.

4. Discussion

[14] This catastrophic loss of tidal energy to small-scale subharmonic motions suggests two immediate questions: what is the dynamical explanation for energy loss from the tide? and why is it localized at this particular latitude?

4.1. Dynamics of Instability Growth

[15] We gain insight into the first question by bandpassing model output near 28.9 degrees into low-mode tidal motions and high-mode subharmonic motions, which together reconstitute over 95 percent of the total energy. Kinematically, most (2/3) of the energy transfer from the propagating tide to the growing instability comes from just one of the nonlinear terms in the energy tendency equation:

$$\frac{\partial E_{\text{sub}}}{\partial t} \approx -v_{\text{sub}} \times v_{\text{sub}} \times \frac{\partial V_{\text{tide}}}{\partial y} \qquad (2)$$

The phase of the instability is such that northward velocity of subharmonic motions, v_{sub}, is in phase with meridional gradients in tidal velocity, V_{tide} (Figure 2, top). The result is that the triple product in (2) is generally positive (Figure 2,

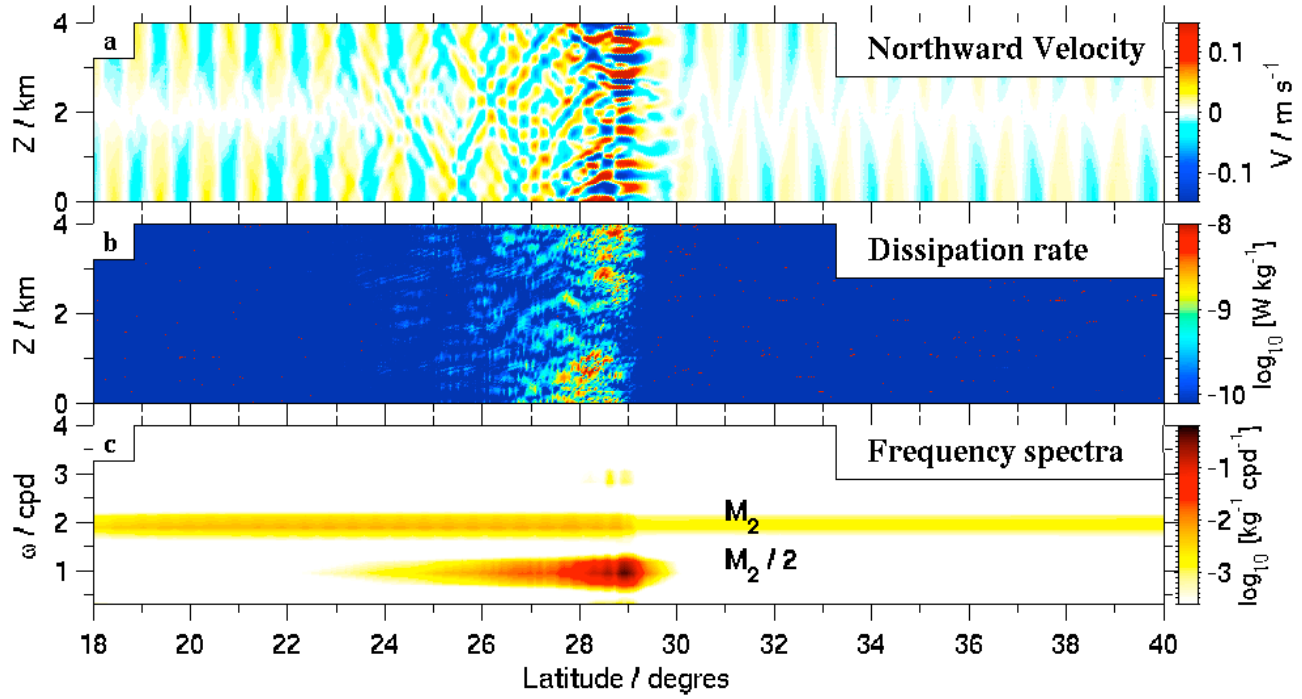

Figure 1. a) Snapshot of northward horizontal velocity (v) after the simulation has reached near steady-state; b) dissipation rate; c) energy spectral density as a function of frequency and latitude. Note that the low-latitude forcing region and high-latitude sponge layers are outside of the domain range shown.

middle). Physically, significant energy transfer occurs whenever the tidal velocity is convergent. When the subharmonic velocity is northward, advection of northward velocity from the tide adds to the northward flow. One tidal period later the subharmonic velocity is southward, and advection of convergent tidal velocity accelerates southward subharmonic flow. In this scenario, vertical motions and restoring forces due to buoyancy play no role.

[16] Once a steady state is reached, energy transfer from the sum of (2) and the similar term $[u_{sub}\ v_{sub}\ dU_{tide}/dy]$ is balanced by local dissipation and divergence of the southward near-inertial energy flux (Figure 2, bottom). In the regions of strongest instability growth (near the critical latitude and either the surface or bottom), the energy transfer rate is approximately 2×10^{-8} W kg^{-1}. The characteristic rate of energy transfer in these regions is consistent in magnitude with a simple dimensional scaling of the relevant nonlinear term,

$$\frac{1}{\tau_{transfer}} \equiv \frac{1}{E_{sub}} \frac{\partial E_{sub}}{\partial t} \sim |V_{tide}|\,|l_{tide}| \approx 10 \text{ days}^{-1}, \qquad (3)$$

where V_{tide} and l_{tide} are characteristic velocity magnitudes and northward wavenumbers of the mode-one tide.

[17] Note that this time scale ($\tau_{transfer}$) characterizes the rate at which energy is transferred from motions at M_2 to those at $M_2/2$ once the flow becomes approximately steady. This is not equal to the time it takes for the instabilities to grow to finite amplitude. As for many idealized studies of instabilities, this second time scale depends sensitively on the energy level and spectral content of the initial perturbations to the background flow.

4.2. Catastrophic Latitudes

[18] The localization of instability growth at 28.9° is related to the fact that subharmonic motions at this latitude are near-inertial, with vanishing vertical velocities and

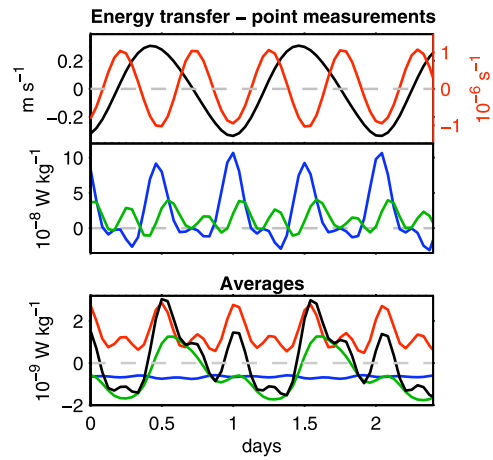

Figure 2. Top panel: bandpassed time series at a particular point in space near 28.9°N of the northward subharmonic velocity (black, left axis) and meridional gradient of northward tidal velocity (red, right axis). Middle panel: subharmonic energy gain through horizontal advection of tidal velocity gradients from term (2), blue, and the similar term $-u_{sub}\ v_{sub}\ dU_{tide}/dy$, green. Bottom panel: a comparison of energy tendency terms averaged over all depths from 28.3 to 29.4°N - the sum of the two energy transfer terms from the panel above (red), dissipation rate (blue), divergence of meridional subharmonic energy flux (green), and the sum of these terms (black).

energy flux. At least two effects limit the growth of instabilities at lower latitudes. First, the vertical group velocity of small-scale subharmonic motions increases with distance south of the critical latitude (as the subharmonic is increasingly super-inertial). For example, at 27°, an instability with similar vertical wavenumber has a vertical group velocity of 3.7×10^{-4} m s^{-1} - hence energy can travel hundreds of meters vertically on a ten-day timescale. Energy flux divergences drain subharmonic energy as it is generated, preventing the exponential buildup possible at the critical latitude. Second, at lower latitudes the energy tendency balance is not as simple as that in equation (3). Additional terms stemming from vertical velocity, displacements, and buoyancy anomalies of the subharmonic waves play significant roles. Analysis of the full energy tendency equation shows that the additional terms act destructivley, reducing the overall growth rate of the subharmonic. The net consequence of these effects is that while PSI may occur at all latitudes south of 28.9° [*Nagasawa et al.*, 2002; *Carter and Gregg*, 2005; *Rainville and Pinkel*, 2005a], it is most efficient close to the critical latitude.

4.3. Caveats and Uncertainties

[19] Several issues arise in considering the implications of our idealized results for the real ocean:

[20] • In an ocean with realistically surface-intensified stratification, horizontal tidal motions are skewed towards high velocities near the surface and weak velocities at depth. The subharmonic instabilities shown here, which draw their energy from horizontal tidal velocity, may consequently also be larger near the surface.

[21] • The approximately ten-day timescale estimated for $\tau_{transfer}$ suggests that neglected processes with comparable time scales could potentially act to disrupt the growth of instabilities. For example, mesoscale variability, both spatial and temporal, is expected to affect the propagation, and therefore, possibly, the fate of internal tides [*Rainville and Pinkel*, 2005b].

[22] • Additional experiments not presented here demonstrate sensitivity to the energy level of the internal tide. Repeating the experiment with half (double) the tidal amplitude results in weaker (stronger) instabilities that allow a greater (lesser) percentage of the northward tidal flux to penetrate past the critical latitude. The strength and consequences of subharmonic instabilities may therefore vary significantly between regions with different tidal fluxes and even at a single location over a spring-neap cycle.

[23] • Finally, care should be taken in interpreting the dissipation rates presented here. The catastrophic instabilities are not well resolved in the sense that by increasing the resolution the vertical scale at which the instabilities occur decreases. The steady-state dissipation rate, however, changes only slightly.

5. Conclusions

[24] We have identified a potentially important physical mechanism of energy loss from a propagating low-mode internal tide using idealized numerical simulations. Near a critical latitude of 28.9°, the modeled internal tide rapidly loses energy to small scale subharmonic motions, which are near-inertial at this latitude. This subharmonic instability extracts energy from lateral gradients in horizontal tidal velocities, and hence is largest near the surface and bottom where mode-one tidal velocities are largest. The high subharmonic shears suggest that large local energy dissipation rates are likely. It is particularly interesting to note that, unlike most discussion of abyssal tidal dissipation in the literature, the surface-intensified turbulence produced by this instability may be important to upper ocean mixing. The instability acts as an effective filter of northward tidal propagation, greatly reducing the baroclinic tidal energy available for mixing poleward of this latitude.

[25] Oceanic realization of such strong, latitudinally localized parametric subharmonic instabilities will likely be limited by several complicating factors not addressed by this idealized study. Numerical [*Merrifield and Holloway*, 2002; *Simmons et al.*, 2004b], historical in-situ [*Rudnick et al.*, 2003] and satellite observations [*Kantha and Tierney*, 1997; *Ray and Cartwright*, 2001] suggest that baroclinic tidal energy radiates away from generation sites in the form of relatively narrow ''beams''. A strong subharmonic signal is hence only expected at longitudes where tidal beams cross the critical latitude (H. Simmons, personal communication, 2005), and thus may not be easily visible in historic observations. Nevertheless, it is encouraging that the location of predicted tidal energy loss is roughly in agreement with some published satellite observations of internal tide propagation. Further numerical and observational work would help to resolve these issues.

[26] **Acknowledgments.** We have enjoyed and benefited from discussions with Walter Munk, Harper Simmons, Matthew Alford, Jody Klymak, and Rob Pinkel. Comments from two reviewers were also helpful in clarifying the paper. This work was sponsored by NSF (OCE 0242471 and OCE 0425283).

References

Carter, G. S., and M. C. Gregg (2005), Persistent near-diurnal internal waves observed above a site of M_2 barotropic-to-baroclinic conversion, *J. Phys. Oceanogr.*, in press.

Dushaw, B. D., B. D. Cornuelle, P. F. Worcester, B. M. Howe, and D. S. Luther (1995), Barotropic and baroclinic tides in the central North Pacific Ocean determined from long-range reciprocal acoustic transmissions, *J. Phys. Oceanogr.*, *25*, 631–647.

Gregg, M. (1998), Estimation and geography of diapycnal mixing in the stratified ocean, in *Physical Processes in Lakes and Oceans*, *Coastal Estuarine Sci.*, vol. 54, edited by J. Imberger, pp. 305–338, AGU, Washington, D. C.

Hasumi, H., and N. Suginohara (1999), Effects of locally enhanced vertical diffusivity over rough bathymetry on the world ocean circulation, *J. Geophys. Res.*, *104*, 23,367–23,374.

Hibiya, T., and M. Nagasawa (2004), Latitudinal dependence of diapycnal diffusivity in the thermocline estimated using a finescale parameterization, *Geophys. Res. Lett.*, *31*, L01301, doi:10.1029/2003GL017998.

Hibiya, T., Y. Niwa, and K. Fujiwara (1998), Numerical experiments of nonlinear energy transfer within the oceanic internal wave spectrum, *J. Geophys. Res.*, *103*, 18,715–18,722.

Hibiya, T., M. Nagasawa, and Y. Niwa (2002), Nonlinear energy transfer within the oceanic internal wave spectrum at mid and high latitudes, *J. Geophys. Res.*, *107*(C11), 3207, doi:10.1029/2001JC001210.

Kantha, L., and C. Tierney (1997), Global baroclinic tides, *Prog. Oceanogr.*, *40*, 163–178.

Merrifield, M. A., and P. E. Holloway (2002), Model estimates of M_2 internal tide energetics at the Hawaiian Ridge, *J. Geophys. Res.*, *107*(C8), 3179, doi:10.1029/2001JC000996.

Munk, W., and C. Wunsch (1998), Abyssal recipes II: Energetics of tidal and wind mixing, *Deep Sea Res., Part I*, *45*, 1977–2010.

Nagasawa, M., T. Hibiya, Y. Niwa, M. Watanabe, Y. Isoda, S. Takagi, and Y. Kamei (2002), Distribution of fine-scale shear in the deep waters of the North Pacific obtained using expendable current profilers, *J. Geophys. Res.*, *107*(C12), 3221, doi:10.1029/2002JC001376.

Olbers, D., and N. Pomphrey (1981), Disqualifying two candidates for the energy balance of oceanic internal waves, *J. Phys. Oceanogr.*, *11*, 1423–1425.

Rainville, L., and R. Pinkel (2005a), Baroclinic energy flux at the Hawaiian Ridge: Observations from the R/P FLIP, *J. Phys. Oceanogr.*, in press.

Rainville, L., and R. Pinkel (2005b), Propagation of low-mode internal waves through the ocean, *J. Phys. Oceanogr.*, in press.

Ray, R. D., and D. E. Cartwright (2001), Estimates of internal tide energy fluxes from Topex/Poseidon altimetry: Central North Pacific, *Geophys. Res. Lett.*, *28*, 1259–1262.

Rudnick, D., et al. (2003), From tides to mixing along the Hawaiian Ridge, *Science*, *301*, 355–357.

Saenko, O., and W. Merryfield (2005), On the effect of topographically enhanced mixing on the global ocean circulation, *J. Phys. Oceanogr.*, *35*, 826–834.

Simmons, H., S. Jayne, L. S. Laurent, and A. Weaver (2004a), Tidally driven mixing in a numerical model of the ocean general circulation, *Ocean Modell. 6*, pp. 245–263, Hooke Inst. Oxford Univ., Oxford, U. K.

Simmons, H. L., R. W. Hallberg, and B. K. Arbic (2004b), Internal wave generation in a global baroclinic tide model, *Deep Sea Res., Part II*, *51*, 3043–3068.

St. Laurent, L., and J. Nash (2004), An examination of the radiative and dissipative properties of the internal tides, *Deep Sea Res., Part II*, *51*, 3029–3042.

Winters, K. B., J. A. MacKinnon, and B. Mills (2004), A spectral model for process studies of rotating, density-stratified flows, *J. Atmos. Oceanic Technol.*, *21*, 69–94.

J. A. MacKinnon and K. B. Winters, Scripps Institution of Oceanography, University of California, San Diego, CA 92093, USA. (jmackinn@ucsd.edu)